

Low-Dimensional Molecular Conductors $(\text{Per})_2\text{M}(\text{mnt})_2$, $\text{M} = \text{Cu}$ and Ni : Low- and High-Conductivity Phases

Vasco Gama, Manuel Almeida,* Rui T. Henriques, Isabel C. Santos, Ângela Domingos,

ICEN-LNETI, Departamento de Química, P-2686 Sacavém Codex, Portugal

Sylvain Ravy, and Jean Paul Pouget

Laboratoire de Physique des Solides, Université de Paris-Sud, Bat 510, F-91405 Orsay Cedex, France

(Received: August 27, 1990)

Single crystals of the quasi-one-dimensional conductors $(\text{Per})_2\text{M}(\text{mnt})_2$ (Per = perylene, M = Ni and Cu, mnt = maleonitrile dithiolate or *cis*-2,3-dimercapto-2-butenedinitrile) were prepared by electrocrystallization. In addition to the previously reported β -phase with semiconducting properties ($\sigma_{\text{RT}} \approx 50 \Omega^{-1} \text{cm}^{-1}$, $S_{\text{RT}} = 22 \mu\text{V K}^{-1}$), a second phase with metallic properties, denoted α , was also obtained. The α - and β -phases differ by their crystallographic structure. A temperature-independent superlattice modulation stabilizing the $6b$ periodicity in the chain direction characterizes the β -phases. The crystal structure of the metallic α -phase consists of a close-packed arrangement of uniform stacks of segregated perylene and $\text{M}(\text{mnt})_2$ units. At room temperature, the electrical conductivity along the stacking axis is $\sigma_{\text{RT}} \approx 700 \Omega^{-1} \text{cm}^{-1}$ and the absolute thermoelectric power has a positive value of $S_{\text{RT}} = 35 \mu\text{V K}^{-1}$. Both the Ni and Cu derivatives exhibit a metallic behavior down to 25 and 32 K, respectively, where a metal–insulator transition occurs.

Introduction

The family of organic conductors $(\text{Per})_2\text{M}(\text{mnt})_2$ (Per = perylene and mnt = maleonitrile dithiolate or *cis*-2,3-dimercapto-2-butenedinitrile) has been known for more than 15 years, since the first report of the compounds with M = Ni and Cu as semiconductors by Alcácer and Maki.^{1,2} More recent studies have focused on the members whose transport properties exhibit metallic character (M = Pt, Pd, Au)^{3–7} while the Ni and Cu salts received little attention. As was emphasized earlier,⁶ some members of the family (e.g., M = Pt, Pd) present a unique situation among the low-dimensional conductors due to the coexistence in the same crystalline structure of conducting chains of perylene molecules and chains of $\text{M}(\text{mnt})_2$ with localized magnetic moments.

The need for a thorough understanding of the behavior of all possible members of this family has driven us to reinvestigate the earlier members (M = Ni and Cu), reported as semiconductors, in single crystalline form. Evidence for the existence of two phases in these compounds, based on preliminary transport data, was previously given.^{8,9} In this paper we show that $\text{Per}_2\text{M}(\text{mnt})_2$, M = Ni and Cu, single crystals prepared by electrocrystallization, with crystal structures and metallic behavior similar to the Pt and Pd analogues, can also be obtained, in addition to the semiconducting phases previously reported. We provide structural data for these two phases.

Experimental Section

$(\text{Per})_2[\text{M}(\text{mnt})_2]$, M = Cu and Ni, single crystals were prepared by electrochemical oxidation of perylene in a dichloromethane

solution ($\approx 10^{-2}$ M) containing $(n\text{-C}_4\text{H}_9)_4\text{N}[\text{M}(\text{mnt})_2]$ ($(1-5) \times 10^{-3}$ M).¹ Special care was taken with the previous purification of the starting reagents. Perylene (Sigma) was gradient sublimed (10^{-2} Torr, 110°C) several times, after recrystallization from pentane and chromatography through an alumina–silica column. $(n\text{-C}_4\text{H}_9)_4\text{N}[\text{Ni}(\text{mnt})_2]$ and $(n\text{-C}_4\text{H}_9)_4\text{N}[\text{Cu}(\text{mnt})_2]$ were prepared as described previously.¹⁰ The Ni salt was recrystallized from acetone/diethyl ether and the Cu salt from dichloromethane/ethanol. Dichloromethane (Merck p.a.) was previously distilled, dried with molecular sieves, and passed through an alumina column just before use. The solutions were deaerated with argon.

In the case of M = Ni the electrocrystallization was performed in a two-compartment cell using platinum electrodes and a galvanostatic technique,¹¹ with current densities in the range 2–10 $\mu\text{A}/\text{cm}^2$. Black crystals with metallic shine and typical dimensions $\approx 10 \times 0.10 \times 0.05 \text{ mm}^3$ were collected from the anode compartment after ≈ 5 days and washed with dichloromethane. Elemental analysis gave the following results: C, 68.38; H, 2.57; N, 6.41. Calculated for $\text{NiS}_4\text{N}_4\text{C}_{48}\text{H}_{24}$: C, 68.33; H, 2.87; N, 6.64.

In the case of M = Cu, single crystals could only be obtained by the use of larger current densities in the range 20–50 $\mu\text{A}/\text{cm}^2$. The crystals, equally black and with metallic shine, but usually thinner, $\approx 5 \times 0.02 \times 0.01 \text{ mm}^3$, were collected after about 1 h and washed with dichloromethane. Lower current densities gave a microcrystalline product with elemental analysis more consistent with $[\text{Cu}(\text{mnt})_2] \cdot \text{CH}_2\text{Cl}_2$ as denoted by the following results: C, 25.31; H, 0.50; N, 13.22. Calculated for $\text{CuCl}_2\text{S}_4\text{N}_4\text{C}_9\text{H}_2$: C, 25.21; H, 0.46; N, 13.06. Elemental analysis of the product obtained with the higher current densities still indicates the presence of small amounts of such material as denoted by the following results: C, 63.81; H, 2.83; N, 6.81. Calculated for $\text{CuS}_4\text{N}_4\text{C}_{48}\text{H}_{24}$: C, 67.94; H, 2.85; N, 6.60.

For both the Ni and Cu derivatives, most batches give more than one phase, but due to factors that remain so far uncontrolled, some batches have almost exclusively α - or β -phases, as judged by thermopower measurements performed in many samples (see below). The crystals of both phases are indistinguishable by external appearance. Thermopower characterization is in this case the most expedient way of probing the type of phase of the crystals,

- (1) Alcácer, L.; Maki, A. H. *J. Phys. Chem.* **1974**, *78*, 215.
- (2) Alcácer, L.; Maki, A. H. *J. Phys. Chem.* **1976**, *80*, 1912.
- (3) Alcácer, L.; Novais, H.; Pedroso, F.; Flandrois, S.; Coulon, C.; Chasseau, D.; Gaultier, J. *Solid State Commun.* **1980**, *35*, 945.
- (4) Henriques, R. T.; Alcácer, L.; Pouget, J. P.; Jérôme, D. *J. Phys. C: Solid State Phys.* **1984**, *17*, 5197.
- (5) Henriques, R. T.; Almeida, M.; Matos, M. J.; Alcácer, L.; Bourbonnais, C. *Synth. Met.* **1987**, *19*, 379.
- (6) Alcácer, L. *Mol. Cryst. Liq. Cryst.* **1985**, *120*, 221.
- (7) Domingos, A.; Henriques, R. T.; Gama, V.; Almeida, M.; Lopes Vieira, A.; Alcácer, L. *Synth. Met.* **1989**, *27*, B411.
- (8) Gama, V.; Henriques, R. T.; Almeida, M. In *Proceedings of the NATO-ASI. Lower Dimensional Solids and Molecular Devices, Spetses, Greece 1989*; Metzger, R. M., Day, P., Papavassiliou, G., Eds.; Plenum Press: New York, 1991; p 219.
- (9) Gama, V.; Henriques, R. T.; Almeida, M. *Fysika* **1989**, *21*, 19.

- (10) Davison, A.; Holm, R. H. *Inorg. Synth.* **1967**, *10*, 19.
- (11) Engler, E. M.; Greene, R.; Haen, P.; Tomkiewicz, Y.; Mortensen, K.; Berendzen, J. *Mol. Cryst. Liq. Cryst.* **1982**, *79*, 15.

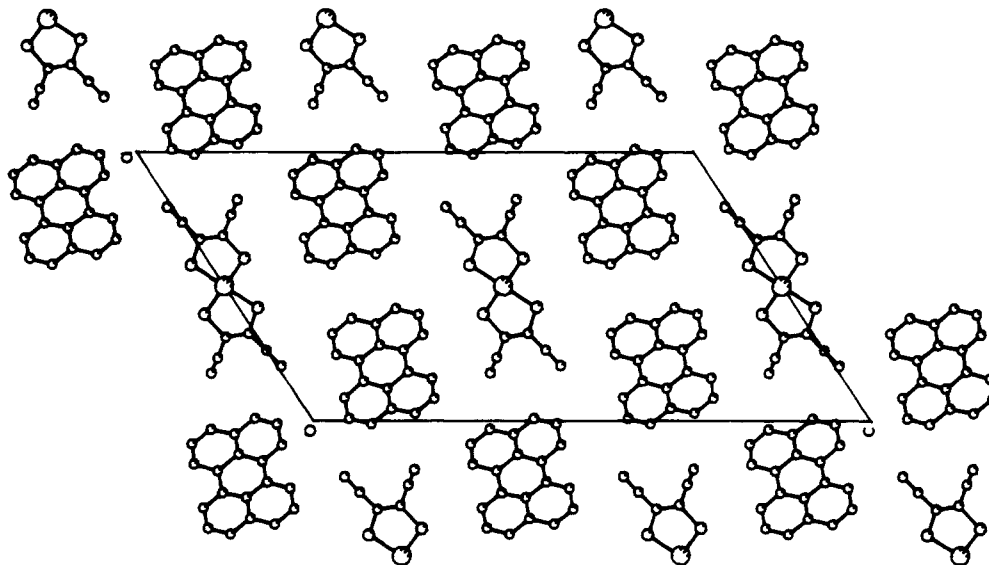


Figure 1. Projection along the b axis of the α -(Per) $_2$ Ni(mnt) $_2$ structure.

introducing only minor damage in the painted extremities of the samples. Elemental analysis in all batches, including those with mostly α - or β -phases, always gave results close to those quoted before and in all cases consistent with a 2:1 stoichiometry. The preparation of these compounds via perylene oxidation with iodine was not extensively used because the crystals obtained, in this way, are usually of poorer quality and possibly contaminated with iodine. Although not so systematically used, the perylene oxidation route with iodine seems to equally give both phases in an uncontrolled way.

A plate-shaped crystal of α -(Per) $_2$ Ni(mnt) $_2$, with dimensions of $0.30 \times 0.04 \times 0.005$ mm 3 , was measured on a Rigaku AFC5R diffractometer with graphite monochromated Cu K α radiation and a 12-kW rotating anode generator in a ω - 2θ scan mode (Molecular Structure Corp.). Data were corrected for Lorentz, polarization, intensity decay (-5.9%), and absorption effects.

The crystals of the β -Ni compound were even of poorer diffracting quality, and in this case, as in the case of the small crystals of the α - and β -phases of $M = \text{Cu}$, Weissenberg photographic techniques using Cu K α monochromatized radiation enabled only the determination of the unit cell parameters. Additional X-ray diffuse scattering experiments were also performed with the so-called "fixed film-fixed crystal" method.

The electrical conductivity along the b axis of the needles was measured in the temperature range 4–300 K, using an in-line four-probe configuration and a low-frequency (77 Hz) current of 1 μ A, the voltage being measured by a lock-in amplifier (EG&G PAR Model 5301). Gold-evaporated contacts were deposited on the sample and were connected to 25- μ m gold wires with platinum paint (Demetron 308). Some measurements performed above 80 K were equally done with contacts made with the conducting paint directly placed on the samples. In all cases special care was taken to select samples with low ($\leq 1\%$) unnested/nested voltage ratios as defined by Schaffer et al.¹² From 300 to 20 K the measurements were done in a closed-cycle cryostat (ADP Cryogenics Inc. HC-2/DE202), and the temperature was monitored by a Au (0.07% Fe)-chromel thermocouple placed close to the sample. For measurements in the range 60 to 4 K, a flux cryostat (Oxford CF204) was used and the temperature was measured with calibrated platinum and germanium resistance thermometers.

The thermopower was measured, along the b axis, relative to gold, in the range 350 to 20 K, by a slow ac technique (10^{-2} Hz) in an apparatus similar to the one described by Chaikin et al.¹³ placed inside a closed-cycle He cryostat or a liquid nitrogen cryostat. The thermal gradients used were ≤ 1 K, and they were

TABLE I: Crystallographic Data of the α -Phases of (Per) $_2$ M(mnt) $_2$ (Space Group $P2_1/c$, $z = 2$)

	M				
	Ni	Cu	Pd ⁷	Pt ³	Au ⁷
a , Å	17.44 (1)	17.5 (1)	16.469 (7)	16.612 (4)	16.602 (2)
b , Å	4.176 (2)	4.17 (2)	4.189 (7)	4.194 (6)	4.191 (1)
c , Å	30.23 (1)	30.6 (2)	30.057 (9)	30.211 (6)	30.164 (3)
β , deg	123.64 (5)	123.5 (5)	118.01 (3)	118.70 (2)	118.69 (1)
V , Å 3	1833 (2)	1860 (40)	1831 (2)	1846.2	1841 (1)

monitored by a Au (0.07% Fe)-chromel thermocouple. The sample temperature was also measured with a Au (0.07% Fe)-chromel thermocouple. Absolute thermopower data were obtained after correction for the small gold absolute thermopower, using the data of Huebner.¹⁴ To avoid possible mistakes and to clearly assign the different behaviors observed in both thermopower and resistivity of the different crystals, present in a particular batch, thermopower was first measured and then, without removing the crystal from the sample holder and by placing two extra voltage contacts, the resistivity was also measured. In this way the resistivity and the thermopower were measured in the same crystal.

Results

The α -phase of the $M = \text{Ni}$ and Cu compounds possesses the monoclinic symmetry, with lattice parameters similar to those of the other metallic members of this series with $M = \text{Au}$,⁷ Pd,⁷ and Pt³ (see Table I). The structure of α -Ni was solved by Patterson and Fourier methods and refined by full matrix least squares¹⁵ to a final $R = 0.126$, $R_w = 0.109$, using 1755 unique reflections, 806 with $F > 2\sigma(F)$. All the perylene carbons and the (mnt) carbons bonded to the sulfur atoms were refined isotropically, and the hydrogen atoms were introduced in the calculated positions. Although with relatively low precision, the solved crystal structure for α -Ni clearly shows segregated regular stacks of perylene and Ni(mnt) $_2$ running along b and in an arrangement similar to the analogues with $M = \text{Pt}$, Pd, and Au.^{3,7} In the unit cell there are four equivalent stacks of perylene molecules and two equivalent stacks of Ni(mnt) $_2$, packed so that each Ni(mnt) $_2$ column is surrounded by six columns of perylene (Figure 1). Although the successive Ni(mnt) $_2$ units are separated by 3.53 Å, with the superposition mode shown in Figure 2, due to their inclination relative to the b axis (32.2°), the distance between consecutive Ni atoms is 4.176 Å. The dihedral angle between the planes of the Ni(mnt) $_2$ units is 64.4°. In each column of perylene, the distance between successive perylene units is 3.37 Å with a su-

(12) Schaffer, P. E.; Wudl, F.; Thomas, G. A.; Ferraris, J. P.; Cowan, D. O. *Solid State Commun.* **1974**, *14*, 347.

(13) Chaikin, P. M.; Kwak, J. F. *Rev. Sci. Instrum.* **1975**, *46*, 218.

(14) Huebner, R. P. *Phys. Rev.* **1964**, *135*, A1281.

(15) Sheldrick, G. M. *SHELX Crystallographic Calculation Program*; University of Cambridge, U.K., 1976.

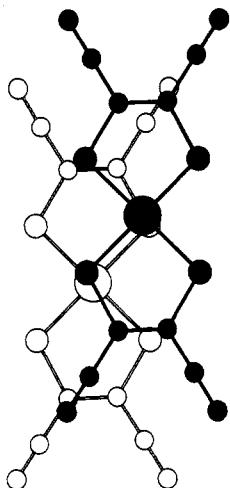


Figure 2. Overlap mode of $\text{Ni}(\text{mnt})_2$ units in $\alpha\text{-(Per)}_2\text{Ni}(\text{mnt})_2$.

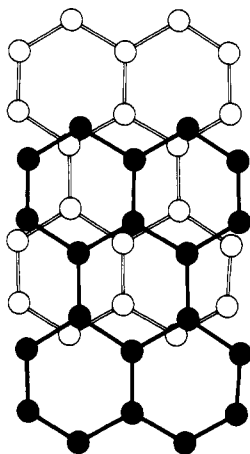


Figure 3. Overlap mode of perylene molecules in $\alpha\text{-(Per)}_2\text{Ni}(\text{mnt})_2$.

TABLE II: Pseudomonoclinic Lattice Parameters of the β -Phase of $(\text{Per})_2\text{M}(\text{mnt})_2$

	M = Ni	M = Cu
a , Å	15.3 (1)	15.3 (1)
b , Å	4.06 (2)	4.07 (2)
c , Å	20.6 (1)	20.8 (1)
β , deg	102.0 (5)	101.5 (5)

perposition mode shown in Figure 3. The inclination of the perylene plane relative to the b axis is 36.1° , and the dihedral angle with the $\text{Ni}(\text{mnt})_2$ units is 24.6° .

For the β -phases, the size and crystal quality did not enable us to perform a structure determination. At most a rough unit cell determination could be performed. Weisenberg photographs are consistent with, as in the previous report of $\beta\text{-Ni}$,¹ a pseudomonoclinic cell. Lattice parameters given in Table II are obtained under this assumption. However, one cannot discard a triclinic lattice symmetry with α and γ deviating slightly from 90° . A recent lattice parameter determination, in a single crystal of $\beta\text{-Ni}$ of better quality, seems to support this latter possibility.¹⁶

A room-temperature X-ray diffuse scattering investigation of $\beta\text{-Ni}$ and $\beta\text{-Cu}$ shows, in addition to layers of Bragg reflections, a set of intense diffuse lines perpendicular to the pseudomonoclinic direction b at the reduced wave vectors $\pm nb^*/6$, with $n = 1, 2$, and 3. They correspond to the establishment of a one-dimensional (1D) superstructure of period $6b$. These lines are all modulated in intensity, which means that there is local order (i.e., in the (a,c) plane) between neighboring $6b$ superstructures. The local ordering does not evolve significantly upon cooling to 30 K. A possible

(16) J. de Boer (private communication) obtains on $\beta\text{-Ni}$: $a = 15.31$ Å, $b = 4.02$ Å, $c = 20.33$ Å, $\alpha = 89.31^\circ$, $\beta = 101.53^\circ$, $\gamma = 93.37^\circ$, and $V = 1224$ Å³.

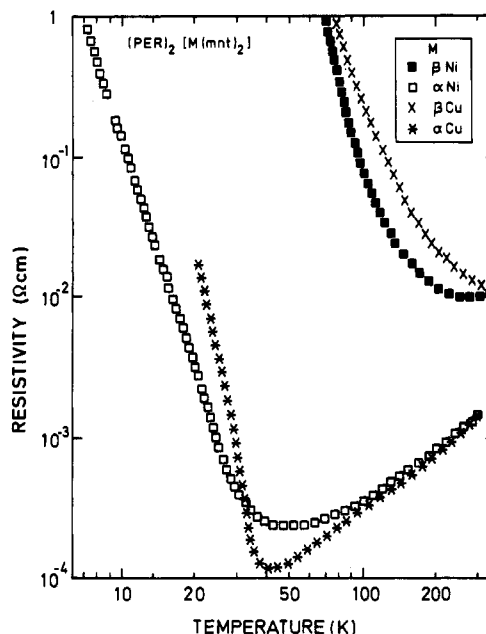


Figure 4. Temperature-dependent resistivity ρ along the b axis of $\alpha\text{-(Per)}_2\text{Ni}(\text{mnt})_2$ (open squares), $\alpha\text{-(Per)}_2\text{Cu}(\text{mnt})_2$ (stars), $\beta\text{-(Per)}_2\text{Ni}(\text{mnt})_2$ (closed squares), and $\beta\text{-(Per)}_2\text{Cu}(\text{mnt})_2$ (crosses).

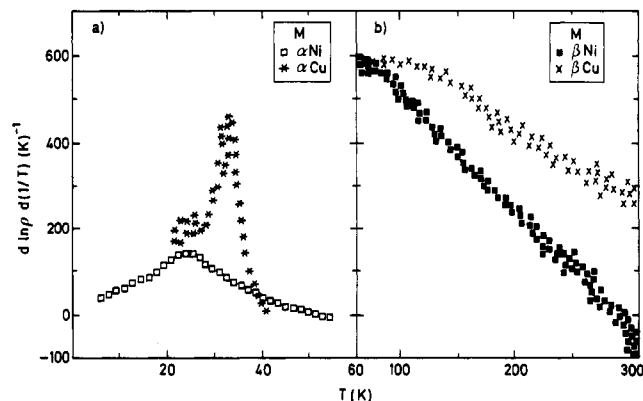


Figure 5. $d \ln \rho/d(1/T)$ plotted as a function of T : $\alpha\text{-(Per)}_2\text{Ni}(\text{mnt})_2$ (open squares), $\alpha\text{-(Per)}_2\text{Cu}(\text{mnt})_2$ (stars), $\beta\text{-(Per)}_2\text{Ni}(\text{mnt})_2$ (closed squares), and $\beta\text{-(Per)}_2\text{Cu}(\text{mnt})_2$ (crosses).

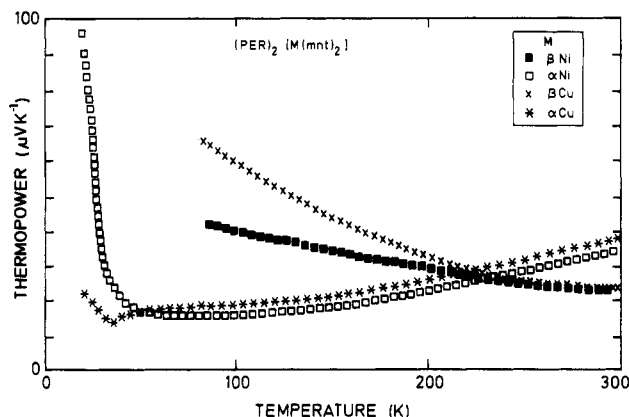


Figure 6. Temperature-dependent absolute thermoelectric power along the b axis of $\alpha\text{-(Per)}_2\text{Ni}(\text{mnt})_2$ (open squares), $\alpha\text{-(Per)}_2\text{Cu}(\text{mnt})_2$ (stars), $\beta\text{-(Per)}_2\text{Ni}(\text{mnt})_2$ (closed squares), and $\beta\text{-(Per)}_2\text{Cu}(\text{mnt})_2$ (crosses).

description of such a superstructure will be given in the Discussion section.

Two distinct types of transport behavior were found in several different crystals, most frequently coming from the same preparation, clearly denoting the existence of the two different phases: one phase with low conductivity ($\sigma(300 \text{ K}) = 50\text{--}90 \Omega^{-1} \text{ cm}^{-1}$) and semiconducting properties similar to those reported earlier,^{1,2}

called β -phase, and another phase described here for the first time, α -phase, with higher electrical conductivity ($\sigma(300\text{ K}) = 500\text{--}800\ \Omega^{-1}\text{ cm}^{-1}$) and metallic properties down to 25 K for $M = \text{Ni}$ and 32 K for $M = \text{Cu}$ where a metal-insulator transition occurs. In all measured samples (more than 20 for each $M = \text{Ni}, \text{Cu}$) we have never observed an intermediate behavior in the transport properties. Typical results of electrical resistivity and thermopower of the α - and β -phases are shown in Figures 4–6.

For the β -phases, the room-temperature conductivity along the needle axis (b) was found to be in the range $50\text{--}90\ \Omega^{-1}\text{ cm}^{-1}$. In the case of $\beta\text{-Ni}$, the resistivity shows a shallow minimum around $250\text{--}260\text{ K}$ depending on the sample and a steeper increase below. No such a minimum was observed in $\beta\text{-Cu}$, where the semiconducting behavior is observed in the whole temperature range below 300 K . In both cases, the activation energy shows a smooth increase upon cooling, reaching values of 90 meV at 100 K (Figure 5). Thermoelectric power in these β -phases was found to be $23\ \mu\text{V K}^{-1}$ for $M = \text{Ni}$ and $22\ \mu\text{V K}^{-1}$ for $M = \text{Cu}$ at room temperature. It increases slightly upon cooling as shown in Figure 6. The rate of increase is however larger for the Cu than the Ni derivative, a behavior consistent with the resistivity measurements.

In the high-conductivity α -phases, the room-temperature conductivity along the needle axis, b , was found to be in the range $500\text{--}800\ \Omega^{-1}\text{ cm}^{-1}$. These values are comparable to those observed in the Pd and Pt analogues where conductivities of ≈ 300 and $\approx 700\ \Omega^{-1}\text{ cm}^{-1}$, respectively, have been reported.^{3,4} As shown in Figure 4, the electrical resistivity exhibits metallic behavior ($d\rho/dT > 0$) at high temperature and presents a minimum at $T_p \approx 50\text{ K}$ in the case of $M = \text{Ni}$ and at $T_p \approx 40\text{ K}$ for $M = \text{Cu}$. Below T_p the electrical resistivity becomes thermally activated, and as shown in Figure 5, there is a metal-insulator transition, better seen through the maximum of $d \ln \rho/d(1/T)$ at 25 K for $M = \text{Ni}$ and at 32 K for $M = \text{Cu}$. The resistivity measurements performed down to 4 K in the case of $\alpha\text{-Ni}$ did not show a constant value for $d \ln \rho/d(1/T)$, and therefore it is not possible to clearly define the energy gap at low temperature. It is estimated to be $\leq 15\text{ meV}$. In case of $\alpha\text{-Cu}$ a constant activation energy was observed, indicating a gap of 20 meV .

In agreement with the resistivity data, thermopower measurements of $\alpha\text{-Ni}$ and $\alpha\text{-Cu}$ (Figure 6) show an almost linear dependence on T at high temperatures, which is also indicative of a metallic behavior. At low temperature, the thermopower varies approximately as $1/T$, a behavior that is typical of a semiconductor. Although not so clearly defined as in the resistivity data, the thermopower, S , in $\alpha\text{-Ni}$ also shows an anomaly of $dS/d(1/T)$ at approximately the same temperature at which the $d \ln \rho/d(1/T)$ anomaly is observed. The room-temperature thermopower was found to be $\approx 38\ \mu\text{V K}^{-1}$ for $\alpha\text{-Cu}$ and $\approx 35\ \mu\text{V K}^{-1}$ for $\alpha\text{-Ni}$. Its positive sign is indicative of a hole-type metallic conduction, as for the β -phases.

Discussion

The main result of the present study is the observation of two different phases of $(\text{Per})_2\text{M}(\text{mnt})_2$ with $M = \text{Ni}$ and Cu . These phases differ by both their structure and electronic properties. The existence of more than one phase with the same composition is not uncommon among low-dimensional organic metals, e.g., in BEDT-TTF salts.¹⁷ For other perylene chain compounds with counterions like ClO_4^- , PF_6^- , or AsF_6^- , different phases have also been reported but associated with different stoichiometries.^{18,19} In the case of perylene with metal-bis(dithiolate) complexes, different stoichiometries have been reported for $M = \text{Pt}$ ²⁰ and $M = \text{Co}$.⁸ In the present compounds, in which both phases have the same composition, the parameters that control whether the α - or

β -phases forms remain unknown.

β -phase crystals show a semiconducting behavior in general agreement with that previously reported by Alcácer and Maki.¹ The main difference is the broad minimum of resistivity observed for $\beta\text{-Ni}$ and not reported by these pioneering authors. In both cases ($M = \text{Cu}$ and $M = \text{Ni}$), the conductivity exhibits a temperature-dependent activation energy also not evident in the previous work.¹ This temperature-dependent activation energy agrees with the observed nonlinear behavior of the thermoelectric power S as a function of $1/T$.

In the absence of a detailed crystal structure description, the origin of the semiconducting properties of the β -phases remains unclear. However, some comments can be made on the basis of the structural data given in the previous section. In particular, the unit cell volume of the β -phase is almost $2/3$ that of the α -phase. As the Per and $\text{M}(\text{mnt})_2$ molecules have comparable volumes, there are four molecules per unit cell. This unit cell is not consistent with a 2:1 stoichiometry between the Per and the $\text{M}(\text{mnt})_2$, if every site is occupied by well-defined molecular species. This means that the unit cell of Table II is that of an average lattice with at least some fractional site occupancy. If there is a local order in site occupancy, a chemical cell of larger volume could thus be formed. It is tempting to associate it with the local superstructure observed by X-ray diffuse scattering. Here we shall only consider the b direction where the diffuse scattering defines more clearly a new lattice periodicity of $6b$. The parameters b of the α - and β -phases are quite close (4.18 and $4.06\ \text{Å}$, respectively), suggesting also the formation of stacks in the β -phase. (The smaller value of b for the β -phase can be due to a reduction of the tilting angle.) It is difficult to understand the periodicity of $6b$ as resulting from a Peierls instability since the critical wave vectors $2k_{\text{F}}^{\text{Per}} = b^*/4$ and $2k_{\text{F}}^{\text{M}(\text{mnt})_2} = b^*/2^4$ are different from $b^*/6$. However, it is interesting to note that $6b$ could be the periodicity of an alternate ordering of tetramers of Per and of dimers of $\text{M}(\text{mnt})_2$. With a transfer of one electron per $\text{M}(\text{mnt})_2$, leaving $1/2$ hole per Per as in the α -phase,⁴ the formation of such entities allows to pair all these charges in singlet states. The ordering of tetrameric and dimeric units along b leads to a 2:1 stoichiometry, whatever the number of stacks per unit cell.

The alternate array of donor and acceptor entities on the stacking direction gives, as for any mixed-charge transfer salts, a semiconducting behavior. However, the transport properties of the β -phase are unusual among low-dimensional organic conductors in the sense that, at room temperature, the electrical conductivity is relatively high for a semiconducting compound. In addition, the thermopower suggests that the carriers are localized holes in the perylene molecules and that transport is via hopping or tunneling between localized states. Such a peculiar feature could be explained by the array proposed, because with a tetramer of Per , which is about 2 times longer than a dimer of $\text{M}(\text{mnt})_2$, a significant interchain overlap between the tetramers wave function, allowing a sizable interstack charge delocalization, could take place. However, the observed interchain disorder will certainly perturbate significantly the conduction path between the tetramer units.

The similarities of the structural parameters among α -phase compounds are consistent with the general similitude of their transport properties. However, in spite of the structural similarities the structure of the α -phase with $M = \text{Ni}$ cannot be considered as isomorphous to that previously found in the compounds with $M = \text{Pt}, \text{Pd}$, and Au , since the tilting angles of the perylene and $\text{M}(\text{mnt})_2$ units toward the b axis are arranged in a reversed way. The structure of the compound with $M = \text{Ni}$ cannot be superposed with those of the compounds with $M = \text{Pt}, \text{Pd}$, and Au . Instead, it corresponds to a mirrorlike arrangement. Two significant differences also concern the angular shift between the molecules and the increase of the β angle. The significant change of the β angle when compared with the analogue compounds is seen as a consequence of the smaller size of the $\text{Ni}(\text{mnt})_2$ unit. By readjustment of the tilting of the molecules and a slight distortion of the unit cell, a tighter packing of the perylene and the $\text{Ni}(\text{mnt})_2$

(17) Williams, J. M.; Wang, H. H.; Emge, T. J.; Geiser, U.; Beno, M. A.; Leung, P. C. W.; Carlson, K. D.; Thorn, R. J.; Schultz, A. J. *Prog. Inorg. Chem.* **1987**, *35*, 51.

(18) Endres, H.; Keller, H. J.; Müller, B.; Schweitzer, D. *Acta Crystallogr.* **1985**, *C41*, 607.

(19) Schweitzer, D.; Hennig, I.; Bender, K.; Endres, H.; Keller, H. J. *Mol. Cryst. Liq. Cryst.* **1985**, *120*, 213.

(20) Shibaeva, R. P.; Kaminskii, V. F.; Simonov, M. A.; Yagubskii, E. B.; Kostiosenko, E. E. *Kristallografiya* **1985**, *30*, 488.

TABLE III: Transport Parameters of (Per)₂M(mnt)₂ α -Phases^a

	M				
	Ni	Cu	Pd	Pt	Au
σ_{RT} , $\Omega^{-1} \text{ cm}^{-1}$	700	700	300	700	700
S_{RT} , $\mu\text{V K}^{-1}$	35	38	32	32	32
T_p , K	50	40	80	18	
T_{M-I} , K	25	32	28	7	
2Δ , meV	<15	20		10	

^a T_p is the temperature of resistivity minimum, T_{M-I} is the temperature of metal-insulator transition, and 2Δ is the low-temperature gap.

chains is allowed. It should be pointed out that the perylene interplanar distance in this case is slightly larger (3.37 Å) than that of the analogues with M = Pd and Au (3.32 Å⁷) and that the superposition mode (Figure 2) shows a small deviation from the graphite-like mode. Also, a noticeable difference with the other analogues is the change of the packing mode of the Ni(mnt)₂ units (Figure 3), allowing the Ni atom to be closer to S atoms of neighboring units.

The structure of the α -phases shows regular stacks of perylene molecules at distances shorter than the sum of the van der Waals radii, indicating electronic delocalization along these stacks. Assuming as for the other members of the α -phase⁴ a charge transfer of one electron toward the M(mnt)₂⁻, there is an average of one hole per two perylene molecules. The positive sign of thermopower is indicative of hole-type conduction and is consistent with metallic conduction in a 3/4 filled band of the perylene chains. Within the tight binding approximation, the thermopower of an uncorrelated one-dimensional metal, neglecting the temperature dependence of the scattering time, is given by²¹

$$S = - \frac{2\pi^2 K_B^2 T \cos(\pi\rho/2)}{3|e|(4t) \sin^2(\pi\rho/2)} \quad (1)$$

where t is the transfer integral between neighboring molecules within a stack ($4t$ is the tight binding bandwidth) and ρ is the number of electrons per site. In spite of the fact that the complete neglect of the Coulomb correlation between electrons is certainly not a very good approximation for this type of molecular solids, the high-temperature thermopower data ($T > 100$ K) can be roughly accounted by eq 1. With $\rho = 3/2$, this enables us to

estimate a bandwidth of $4t = 0.58$ eV. Very similar results have been obtained in the Pt, Pd, and Au analogues with $S_{RT} \approx 32$ $\mu\text{V K}^{-1}$ (see Table III), in agreement with the observed similar stacking mode and interplanar distances of the perylene molecules along the chain axis b in all members of this family. The slightly larger value of thermopower of α -Ni is in agreement with a slightly larger interplanar distance observed between the perylene molecules (3.37 Å for M = Ni when compared to 3.32 Å for M = Au and Pd⁷) and the consequent decrease of the bandwidth.

The general behavior of the transport properties of the α -Ni and α -Cu crystals resembles those observed in the Pt and Pd analogues as shown by Table III. The transport properties of the α -Ni and α -Cu clearly show a metal-insulator transition at 25 and 33 K, respectively. Similar transitions were previously reported in the Pd and Pt compounds.⁴ In these materials it was found that the metal-insulator transition occurring in the perylene stacks is coupled to a structural instability leading to a pairing of the degrees of freedom of the M(mnt)₂ chains. The metal to insulator transition of α -Ni, which also contains magnetic chains, could have the same origin. The detailed mechanism of this transition is however not understood. In this respect, it is interesting to remark that in the case of α -Cu, where the Cu(mnt)₂⁻ unit is diamagnetic, we also observe a clear metal-insulator transition, previously not observed in case of M = Au which also possesses a diamagnetic Au(mnt)₂⁻ counterion. In order to obtain a more clear description of the nature of these transitions, magnetic and X-ray diffuse scattering studies of α -Cu and α -Ni are under way.

In conclusion, the present results show that (Per)₂Ni(mnt)₂ and (Per)₂Cu(mnt)₂ can be obtained in two phases; one phase, β , is semiconducting and adopts a different structural type while the other one, α , is metallic at room temperature and exhibits electronic properties similar to the M = Pd, Pt, and Au analogues.

Acknowledgment. The authors acknowledge Prof. L. Alcácer for stimulating discussions and continuous encouragement. This work was partially supported by EEC under Contract ESPRIT-3121 and by Junta Nacional de Investigação Científica e Tecnológica under Contract 798/90/MPF.

Supplementary Material Available: Tables 1–6 listing atomic coordinates, isotropic and anisotropic thermal parameters, bond lengths, and bond angles for α -(Per)₂M(mnt)₂ (4 pages); tables of calculated and observed structure factors (4 pages). Ordering information is given on any current masthead page.

(21) Kwak, J. F.; Beni, G.; Chaikin, P. M. *Phys. Rev.* 1976, 13, 641.